Planetary- and Synoptic-Scale Influences on Eastern Pacific Tropical Cyclogenesis

JOHN MOLINARI AND DAVID VOLLARO

Department of Earth and Atmospheric Sciences, University at Albany, State University of New York, Albany, New York

(Manuscript received 4 August 1999, in final form 21 February 2000)

ABSTRACT

The structure and evolution of lowpass-filtered background flow and synoptic-scale easterly waves were examined during the 1991 eastern Pacific hurricane season. Active and inactive cyclogenesis periods conformed well to the sign of the near-equatorial, lowpass-filtered, 850-mb zonal wind anomaly, consistent with the recent results of Maloney and Hartmann. This behavior emphasizes the importance of westerly wind bursts associated with the Madden–Julian oscillation (MJO) in creating an environment favorable for eastern Pacific tropical cyclogenesis.

Synoptic-scale easterly waves reached the western Caribbean and eastern Pacific regularly from upstream, usually from Africa. The amplitude of waves leaving Africa had little correlation with the likelihood of a wave producing an eastern Pacific storm. Rather, easterly waves intensified, and tropical depressions formed, during the convectively active phase of the MJO in the western Caribbean and eastern Pacific. Wave growth, measured by strengthening of convection within the waves, occurred in the regions of sign reversal of the meridional potential vorticity gradient found previously. For the 1991 season cyclogenesis occurs when westward-moving synoptic-scale waves amplify within the superclusters that represent the favorable MJO envelope. Analogously, waves existed but failed to grow during the unfavorable part of the MJO.

During each active period of the MJO, the region of active convection moved eastward and northward with time in the eastern Pacific, with strongest convection reaching as far as the southwestern Gulf of Mexico by the end of such periods. The locations of tropical depression formation followed a similar path, shifting eastward with time following the MJO, and northward following the eastern Pacific intertropical convergence zone. The latter was defined by the locations of low-pass-filtered background vorticity maxima at 1000 mb.

It is argued based on previous work in the literature that the western Pacific might behave similarly, with upstream easterly waves growing and producing depressions within the convectively active envelope of the MJO.

1. Introduction

Molinari et al. (1997) proposed that tropical cyclogenesis during the 1991 eastern Pacific hurricane season was strongly controlled by the Madden–Julian oscillation (MJO; Madden and Julian 1994). They noted an excellent correspondence between lowpass-filtered convective heating [measured by outgoing longwave radiation (OLR)], strength of the sign reversal of the meridional gradient of potential vorticity (PV) in the Caribbean and eastern Pacific, and eastern Pacific cyclogenesis. They argued that the dynamic instability implied by the PV gradient sign reversal provided a mechanism relating convective heating in the MJO to subsequent tropical cyclogenesis. By this reasoning either upstream waves were reinvigorated or disturbances developed in situ in the sign reversal region, and tropical depressions formed downstream in the eastern Pacific within these growing waves.

Molinari et al. (2000) considered the development of a single eastern Pacific storm, Hurricane Hernan of 1996. They provided evidence that the pre-Hernan wave grew in amplitude in the western Caribbean and eastern Pacific in the presence of a dynamically unstable background. They argued that processes associated with the growing wave amplitude led subsequently to cyclogenesis. These included (i) an acceleration of southwesterlies at the surface ahead of the wave that produced a stronger intertropical convergence zone (ITCZ), and (ii) strong flow through the Isthmus of Tehuantepec that created a surface vorticity maximum east of the Gulf of Tehuantepec. The tropical depression formed when the 700-mb vorticity center passed over the surface vorticity maximum.

From these two studies it could be argued that wave growth in an environment made favorable by the MJO was by itself a sufficient larger-scale mechanism to account for a significant fraction of eastern Pacific tropical

Corresponding author address: Dr. John Molinari, Department of Atmospheric Sciences, University at Albany, State University of New York, 1400 Washington Ave., Albany, NY 12222.
E-mail: Molinari@atmos.albany.edu

cyclogenesis. If this were true, other factors such as mountain influences (Zehnder 1991; Farfan and Zehnder 1997; Zehnder et al. 1999), wind surges (Zehr 1992; McBride 1995), and the many complex mesoscale interactions that are likely of critical importance in the actual depression development and growth (e.g., Ritchie and Holland 1993; Harr et al. 1996; Bister and Emanuel 1997; Simpson et al. 1997; Raymond et al. 1998; Bracken 1999) would not determine *whether* a tropical cyclone formed, but only the exact timing and location of cyclogenesis within the favorable envelope provided by the MJO and the synoptic-scale wave.

Several uncertainties made this conclusion open to question. The 1991 season contained clear-cut on–off periods of genesis on the MJO timescale, but this is not always so. In addition, Molinari et al. (1997) did not actually provide evidence of wave growth prior to cyclogenesis in the 1991 season. As a result, it was unclear whether the many other proposed mechanisms of eastern Pacific tropical cyclogenesis [see discussions by Molinari et al. (1997, 2000) and general reviews by Frank (1987) and McBride (1995)] might often have an equal or greater role than the MJO-driven process described above.

Recently the picture has cleared somewhat as a result of the work of Maloney and Hartmann (2000, hereafter MH). Maloney and Hartmann defined the phase of the MJO using principal component analysis of the dominant EOFs of the near-equatorial (5°N–5°S), lowpass-filtered (20–80 day), 850-mb zonal wind anomaly in the eastern Pacific. They showed that over a 16-yr interval tropical cyclogenesis was twice as likely during periods of large westerly wind anomalies than periods of large easterly anomalies. In addition, tropical cyclones were much stronger on average and hurricanes were more than four times as likely during such favorable periods. They attributed this outcome to the presence of greater MJO-induced cyclonic shear vorticity in the lower troposphere during active periods, consistent with the arguments of Gray (1979). The magnitude of the vorticity anomalies was comparable to those between developing and nondeveloping disturbances found by McBride and Zehr (1981). Maloney and Hartmann argued that atmospheric Kelvin wave–related flow anomalies associated with the MJO were the fundamental mechanism by which the cyclonic background flow was produced. Enhanced tropical cyclogenesis during the favorable phase of the MJO has been described in the western Pacific as well, by Yamazaki and Murakami (1989), Liebmann et al. (1994), and Hartmann et al. (1992). In contrast, the global anomaly fields of MH showed no lower-tropospheric MJO influence over ocean in the Atlantic basin, other than in the Gulf of Mexico and the western Caribbean, suggesting that most Atlantic storms form by quite different mechanisms.

E. D. Maloney and D. L. Hartmann (1999, personal communication) have argued that the flow structure during active periods in the eastern Pacific favors barotropic conversion of mean flow kinetic energy to eddy kinetic energy, thus creating growing waves that are more likely to produce tropical depressions. Their arguments, and those of Sobel and Bretherton (1999), favor nonmodal growth rather than the modal instability postulated by Molinari et al. (1997). In either case, the active MJO is producing a background field favorable for eddy growth.

Maloney and Hartmann (2000) showed that the MJO modulates eastern Pacific cyclogenesis not just occasionally, as in the 1991 season, but persistently over the 16 yr of their composites. They did not address the possible role of already existing waves from upstream. Also, they showed composited behavior but not the time evolution during a particular season. Finally, the vorticity anomalies they show bring into question the role of the ITCZ, if any, in the cyclogenesis process. Tomas and Webster (1997) show a well-defined mean ITCZ in the eastern Pacific, but MH's results suggest that the flow fluctuates between two distinct extremes. The meaning of the ITCZ, its relationship to MJO fluctuations, and its time evolution are uncertain.

In light of the MH results, we are returning to the 1991 eastern Pacific hurricane season in this paper. The goals are to address the roles of upstream waves and the ITCZ, and to show the time evolution during the season as the eastward-moving MJO interacts with westward-moving waves.

TABLE 1. Tropical depression formation in the eastern Pacific during 1991 for the period covered by this study. Information is taken from the best-track file at the National Hurricane Center. The time given is the first 6-hourly time during which a depression existed, and the location is given for that time.

Storm	Genesis day	Hour (UTC)	Latitude (°N)	Longitude (°W)
Blanca	14 Jun	1800	10.2	103.0
Carlos	16 Jun	1200	11.4	95.4
Delores	22 Jun	1200	12.6	101.1
Trop. depr. 5	28 Jun	1200	12.7	92.9
Enrique	15 Jul	1200	9.4	111.9
Fefa	29 Jul	0600	10.8	107.2
Guillermo	4 Aug	0000	12.3	98.4
Hilda	8 Aug	0000	13.3	101.9
Trop. depr. 10	12 Sep	1200	17.0	106.7
Ignacio	16 Sep	0600	14.1	102.2
Jimena	20 Sep	1800	10.1	100.1
Kevin	25 Sep	0000	12.2	96.2
Linda	3 Oct	1200	13.4	108.7
Marty	7 Oct	1200	12.2	95.3

2. Data sources

Table 1 gives the name, date, and location of each depression formation for 1991 eastern Pacific storms of interest in this study. In addition to depressions associated with 11 named tropical cyclones, this study includes tropical depressions 5 and 10 that did not reach storm strength. Because the values in Table 1 are taken from the best-track data of the National Hurricane Cen-

ter, available at 6-h intervals, the positions and times of depression formation are those at the first 6-hourly time after actual formation. The potential 3-h errors in actual time and position of genesis will be insignificant in this study, in which the timescales of interest are more than an order of magnitude larger.

Molinari et al. (1997) defined 1991 seasonal mean fields over the time period 15 June–30 September. In order to fully encompass the major periods of active cyclogenesis, the definition of the seasonal mean will be slightly altered in this paper to encompass 1 June–15 October. Only two 1991 storms are not included in this study, one in May and one in November.

Gridded analyses from the European Centre for Medium-Range Weather Forecasts (ECMWF) will be used for some calculations. In previous work (Molinari and Vollaro 1990; Molinari et al. 1992, 1997, 2000) extensive discussion of the benefits and limitations of these analyses has been given. Molinari et al. (2000) noted that because of the lack of data in the eastern Pacific, individual case studies should not be undertaken unless the analyses meet a number of criteria involving time continuity, timing and location of tropical depression formation, and consistency with independent datasets such as OLR. These criteria were met for the pre–Hurricane Hernan case study of Molinari et al. (2000), but often they are not met in this region of the globe. In the current study of an entire season, synoptic-scale disturbances will be of interest only in a bulk sense, that is, whether disturbances are frequent or infrequent, and strong or weak, during a particular time period; no fine details of disturbances will be examined. In addition, some information on easterly wave activity will be determined from directly measured OLR data.

OLR data are available twice daily on a 2.5° latitude–longitude grid (Gruber and Winston 1978) and contain the improved interpolation for missing data of Liebmann and Smith (1996). Because the OLR data are measured from polar-orbiting satellites, they only crudely capture the diurnal variation at any given point. In addition, the diurnal signal can sometimes mask wave signatures over and near land areas. For these reasons, the data are filtered to keep only periods 2 days and above, consistent with Raymond et al. (1998) and Molinari et al. (2000).

Lowpass and bandpass time filters follow the methods described by Molinari et al. (1997). The lowpass filter has a cutoff of 20 days, and will be interpreted as the slowly varying background state. The 2–6-day bandpass filter will be interpreted as the easterly wave scale. Lowpass anomaly fields are calculated by subtracting the seasonal mean from the lowpass-filtered fields. In practice these lowpass anomalies are nearly equivalent to the 20–80-day anomalies shown by MH. One change has been made from Molinari et al. (1997): the number of time periods used in the filtering has been nearly doubled to 241, thereby sharpening the response considerably for the lowpass filter.

Part of this paper deals with the evolution of the ITCZ during active periods. The ITCZ is highly transient on a day-to-day timescale; it is often not possible to define a simply connected feature in OLR or vorticity. This is perhaps not surprising given the inherent instability of the ITCZ postulated by Schubert et al. (1991). In this paper the ITCZ position at each longitude will be defined primarily by the latitude of lowpass-filtered 1000-mb relative vorticity maxima. The maxima are chosen only from points north of the equator over ocean. The lowpass-filtered vorticity evolution in the gridded analyses carries much greater confidence than, for instance, day-to-day variations. If it is assumed that five data points are required to adequately define a wave over one period, then a 20-day oscillation requires only one data value every 4 days, whereas a 3-day oscillation essentially requires two observations per day. The frequent presence of cloud track winds and other nonconventional data sources in the global analyses suggests that the lowpass background fields should be well represented.

The ITCZ will also sometimes be described in terms of lowpass-filtered OLR minima. It will be shown that, for time-averaged and composite fields, such a measure gives similar information to the 1000-mb vorticity described above. When the time variation of the ITCZ is considered, however, lowpass OLR minima cover such a large region that no ITCZ is easily identifiable. Only lowpass vorticity fields will be used to define the time variation of the ITCZ. The reason for the inconsistency is not certain; rather it reflects general uncertainty in our knowledge of the ITCZ.

The final potential complication in the ITCZ definition occurs because eastern Pacific tropical cyclone formation varied strongly on the MJO timescale during 1991 (Molinari et al. 1997). As a result, the possibility exists for aliasing tropical cyclone OLR and vorticity into the lowpass-filtered fields. This obviously complicates the conceptual separation of disturbance and background and, thus, complicates the definition of the ITCZ. This issue will be addressed further in sections 3 and 5.

3. Planetary-scale influences on eastern Pacific cyclogenesis

Figure 1 shows a latitude–time series of the lowpass-filtered 850-mb zonal wind anomaly from 4.5°S to 20.25°N, averaged over the region 90.0°–120.375°W. The part of this region from 4.5°S to 4.5°N corresponds, within the resolution of the gridded analyses, to that used by MH to distinguish the phase of the MJO life cycle. The three active periods, defined as having a westerly zonal wind anomaly averaged from 4.5°S to 4.5°N, are indicated by the pairs of heavy horizontal lines in Fig. 1. Also shown in Fig. 1 are tropical cyclone genesis times, plotted at the nearest 12-h tick mark.

It is apparent that the 1991 season follows well the findings of MH, even though the MJO in Fig. 1 has

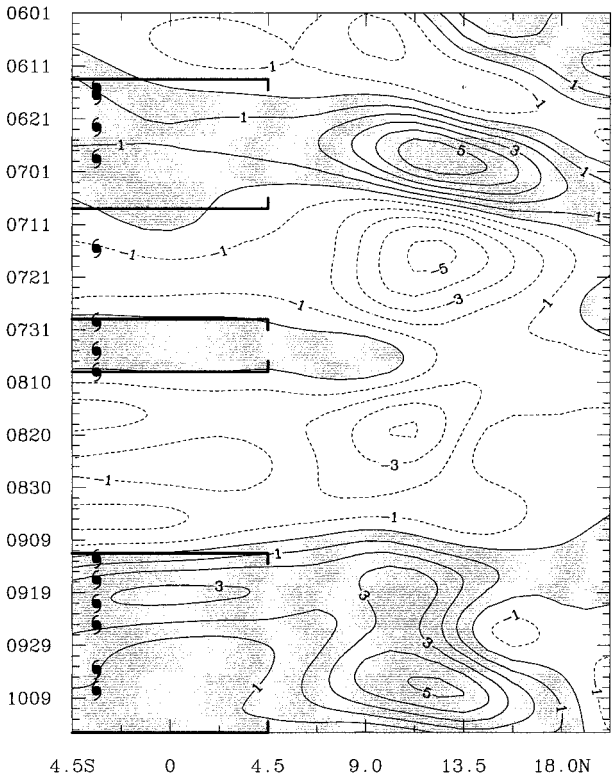

FIG. 1. Latitude–time series of the lowpass-filtered 850-mb zonal wind anomaly averaged between 90.0° and 120.375°W. The contour increment is 1 m s^{-1} and positive values are shaded. The heavy solid lines bracket each of the active periods, defined by the sign of the zonal wind anomaly 4.5°S–4.5°N following MH. The tropical cyclone symbols indicate the times (to the nearest 12 h) of tropical depression formation in the eastern Pacific.

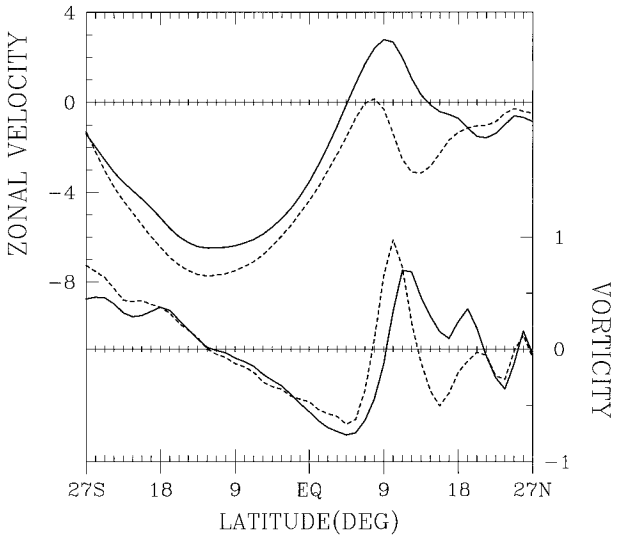

FIG. 2. Composited 1000-mb zonal velocity (m s^{-1}) and relative vorticity (10^{-5} s^{-1}), averaged between 90.0° and 120.375°W, for active periods (solid) and inactive periods (dashed). Active and inactive periods are defined as in Fig. 1. Each tick mark on the horizontal axis represents 1.125° latitude.

been divided into only two phases. All but one of the 13 depressions occurred during an active period when the near-equatorial lowpass zonal wind anomaly at 850 mb was from the west. The full x–y variation of the lowpass active and inactive 850-mb wind anomalies (not shown) also closely resembled that of MH.

Figure 1 shows that the lowpass anomaly u component is much larger between 10° and 14°N than at the equator, consistent with the results of MH. Ferreira et al. (1996) showed that if a heat source representing the MJO were shifted off the equator, the maximum westerly anomaly shifted in the same direction. In the eastern Pacific, cold water at the equator strongly suppresses convection and thereby creates an off-equatorial heat source. The simulations of Ferreira et al. (1996) suggest that this cross-equatorial asymmetry in heating produces a shift of the largest zonal wind anomaly to well north of the equator.

In this paper the structure of the ITCZ will also be investigated. Figure 2 shows the zonal wind and relative vorticity structure at 1000 mb for the composite active and inactive periods, averaged from 90.0° to 120.375°W, the same region chosen by Tomas et al. (1999). Because active times are slightly more frequent than inactive times during the period in question, the mean field lies nearly but not exactly halfway between the two composites. The seasonal mean ITCZ for 1991 (not shown) lies at 11.25°N and has a structure similar to that given by Tomas et al. (1999).

Figure 2 shows that near-surface monsoon westerlies are almost completely absent during inactive periods, but extend northward across 1000 km of latitude during the active periods. During inactive periods the ITCZ, defined by the 1000-mb vorticity maximum, lies at 10.125°N, and the region of cyclonic vorticity extends only about 500 km in latitude. During active periods cyclonic vorticity extends much farther northward. Nevertheless, the composite ITCZ shifts only about 200 km northward during such periods and weakens slightly.

The composite v component of the wind at 1000 mb (not shown) is almost identical for active and inactive periods. The largest northward motion occurs just poleward of the zero absolute vorticity contour (consistent with Tomas and Webster 1997), which itself lies at almost the identical latitude for both active and inactive composites. The lack of change in the meridional wind between active and inactive periods emphasizes the convectively coupled, Kelvin wave–like nature of the MJO, as noted by MH.

Figure 3 shows composite OLR fields for active and inactive periods, and their difference. Consistent with the vorticity composites described above, the region of active convection (given approximately by OLR < 210 W m^{-2}, shaded in Fig. 3) expands northward and covers a much larger area during active periods. Nevertheless, during both active and inactive periods, the ITCZ, as measured by the OLR maxima at each longitude, is

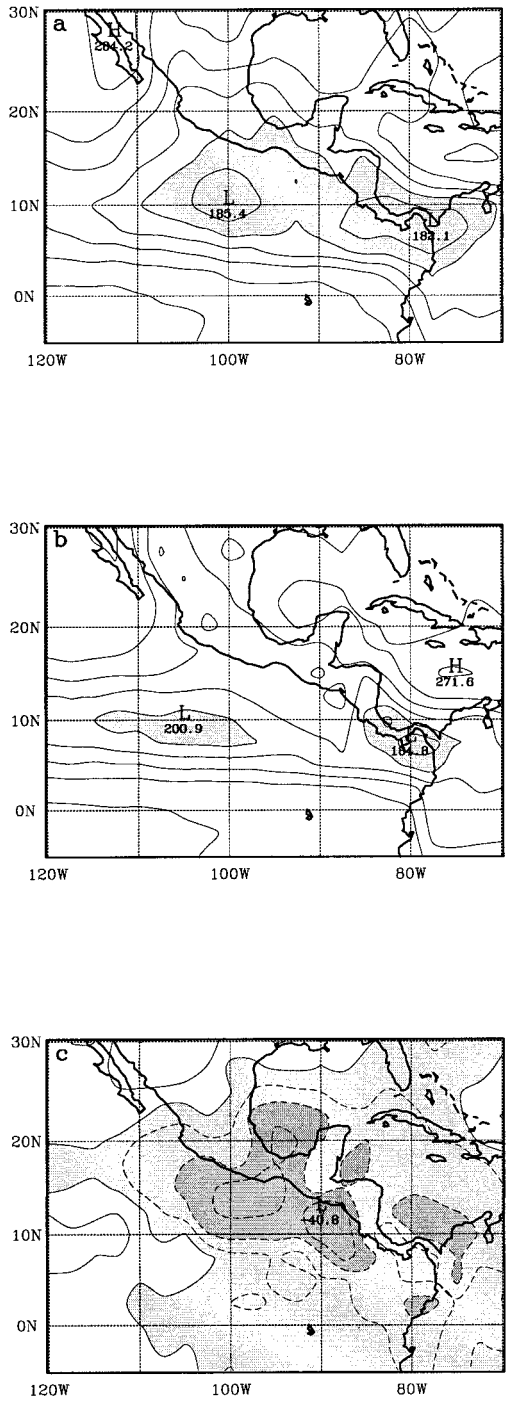

FIG. 3. Composited outgoing longwave radiation (W m^{-2}), filtered to remove the diurnal oscillation, for (a) active periods, (b) inactive periods, and (c) difference between active and inactive. Active and inactive are defined as in Fig. 1. (a), (b) Contour increment 15 W m^{-2} and (c) 10 W m^{-2}. Shading in (a) and (b) indicates OLR < 210 W m^{-2}. In (c), light and dark shading indicate an OLR anomaly between 0 and -20 W m^{-2} and < -20 W m^{-2}, respectively.

nearly zonally oriented along 10°N, with a southward turn to 8°N near Panama. The difference field (Fig. 3c) closely resembles the composite precipitation anomalies of MH. Figure 3 also has a strong resemblance to the precipitation anomalies during the Mexican rainy season and ''midsummer drought'' shown by Magaña et al. (1999). The implication is that the MJO also influences such drought and rainy periods over Mexico.

The stronger convection west of 95°W in Fig. 3c could arise from the presence of tropical cyclones, but the stronger convection to the east suggests the possibility that waves in the easterlies are more convectively active during periods of frequent cyclogenesis, as would be expected if depressions form in association with such waves. The enhanced convection during the composite active period extends to the western Caribbean and through the Isthmus of Tehuantepec to the far southwest Gulf of Mexico.

The definition of the ITCZ is somewhat unclear in the composite OLR fields. The maximum convection occurs at similar latitudes in the active and inactive composites. If one defines the ITCZ in the composites by the latitude of maximum convection, Fig. 3c shows that the major increase in convection during active periods occurs north of the mean ITCZ. The composite fields might disguise considerable transience and extensive meridional oscillation of the ITCZ. Alternatively, the ITCZ may stay in place, and tropical cyclones may form from waves that remain north of the ITCZ.

In order to address this issue further, Fig. 4 shows the time evolution of lowpass-filtered OLR and 1000-mb relative vorticity before (Fig. 4a), during (Figs. 4b–e), and after (Fig. 4f) the first active period. The lowpass-filtered OLR is contoured directly, while vorticity is indicated by plotting a symbol at the latitudes of its maxima in the eastern Pacific, as described in section 2. The locations of tropical depression formations are also shown for a 1-week period centered on the time of each panel in the figure.

At the initial time (0000 UTC 8 Jun; Fig. 4a) the ITCZ, defined by lowpass-filtered OLR minima and ζ_{1000} maxima, is nearly zonally oriented along 9°–10°N. The first two depressions form during the following week (Fig. 4b). During this time the deep convection extends eastward and northward. Maximum low-level vorticity shifts northward near 100°W with the convection. The ITCZ seems clearly defined across the entire region from 115° to 70°W by the strip of deep convection (OLR $<$ 210 W m^{-2}; dark shading). After this time, however, the region of deep convection is so large during the active MJO that OLR provides little insight into the position and motion of the ITCZ.

By 22 June (Fig. 4c), deep convection has spread farther northward and eastward and now includes the southwest Gulf of Mexico and the western Caribbean. The maximum vorticity has shifted northward with the convection in a region centered on 100°W. Farther west, toward cooler water at 110°W, neither the OLR mini-

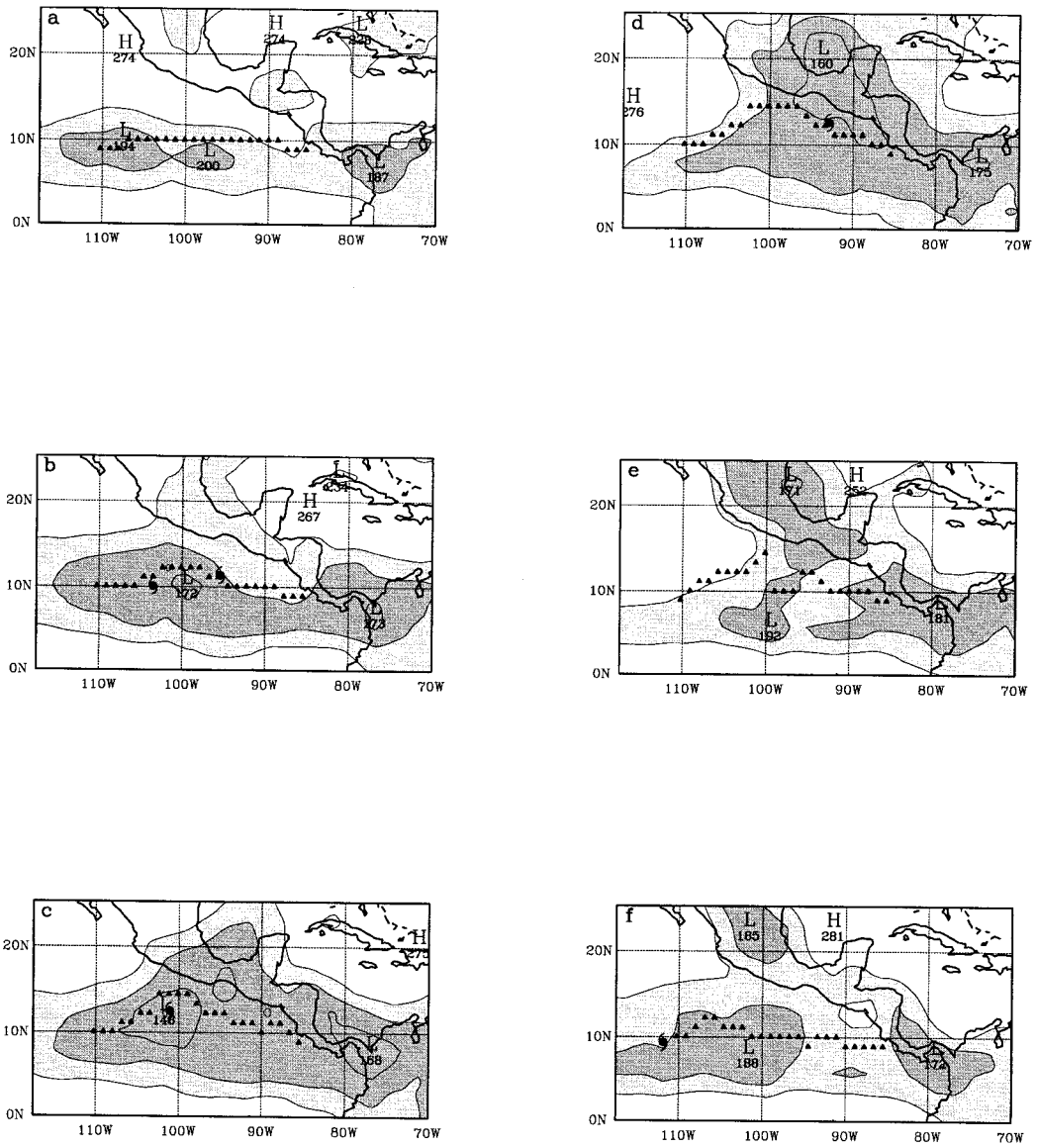

FIG. 4. Lowpass-filtered OLR (W m^{-2}) and latitudes of 1000-mb vorticity maxima before and during the first active period, which began 14 Jun 1991 and ended 8 Jul 1991. The triangles indicate the position of the lowpass-filtered 1000-mb vorticity maximum over water at each longitude. The OLR contour increment is 30 W m^{-2}; only contours less than or equal to 240 W m^{-2} are shown. Shading represents 210–240 W m^{-2} and $<$210 W m^{-2}, respectively. The fields are displayed at 0000 UTC for the following dates: (a) 8 Jun, (b) 15 Jun, (c) 22 Jun, (d) 29 Jun, (e) 6 Jul, and (f) 13 Jul.

mum nor the the ζ_{1000} maximum have moved significantly. By 29 June (Fig. 4d) deep convection is weakening at the western end while continuing to expand northward and eastward; the latter would be expected on this timescale as the MJO shifts eastward. The deepest convection during this late part of the active period is no longer in the eastern Pacific, but rather is in the southern Gulf of Mexico. Deep convection is also well defined along the Andes down nearly to the equator. The last eastern Pacific tropical depression of the active period formed during this week. It formed near the Mexican coast east of the Gulf of Tehuantepec, consistent with the northward and eastward shift of depression formation during the period. During the entire active period, every tropical depression formed near the local ITCZ position as defined by the lowpass-filtered 1000-mb vorticity maxima.

By 6 July (Fig. 4e), at the end of the active period using the MH definition, deep convection is weakening throughout. There appears to be no systematic shift of the ITCZ back southward, but rather a general breakup of convection. Both the convective maxima and ζ_{1000}

maxima are irregular, with some indication of a reformation of the ITCZ near and south of 10°N. By 13 July (Fig. 4f) the ITCZ has nearly returned to its preactive period position south of 10°N. A depression formed during this week that does not meet the MH active period criterion. Later it will be suggested that this is part of the next active period, in which depressions again begin to form well to the south and west. Once again the depression forms near the lowpass-filtered ITCZ location.

Overall, the planetary scale appears to have exerted strong control on tropical cyclogenesis in the eastern Pacific during 1991. All but one depression developed during a time the equatorial lowpass 850-mb zonal wind anomaly was from the west, indicative of an active MJO (MH). The time sequence showed that convection spread eastward as expected during the active period, but also spread northward. The reason for the northward extension of convection in an eastward-propagating Kelvin wave is uncertain. It might represent an edge wave along the Central American mountains produced after the lower-tropospheric Kelvin wave reaches the Andes (Matthews et al. 1999; Weickmann et al. 1997).

The ITCZ in the lowpass-filtered fields appears to shift northward during the active periods in both the OLR and vorticity fields. As noted earlier, the tropical cyclones could be aliased into the lowpass-filtered fields. In the worst-case scenario, the ITCZ actually moved little and the northward shift was simply the aliasing of OLR minima and vorticity maxima of the cyclones into the lowpass fields. It cannot be said with certainty that this is not the case. However, the tropical cyclones continue to represent vorticity maxima and OLR minima as they move northward and westward from their formation region, and there is little indication of these tracks (see Rappaport and Mayfield 1992) in the Fig. 4 fields. The evidence suggests that the ITCZ does experience a northward shift during active periods. This shift parallels that of depression formation, suggesting that tropical cyclones are forming within the ITCZ as it is defined in this paper.

The composite and lowpass-filtered fields shown in Figs. 1–4 do not give any information on synoptic-scale activity. In particular, the behavior of easterly waves during active and inactive periods, and their potential role in genesis, will be examined in the following section.

4. Synoptic-scale influences

Molinari et al. (2000) showed evidence, using 700-mb v-component Hovmöller diagrams, of 2–6-day disturbances from Africa reaching the eastern Pacific and being associated with tropical cyclogenesis during a 1-month period in 1996. Figure 5a shows such a Hovmöller diagram for the 1991 season, averaged between 10.125° and 12.375°N. Also shown are the longitudes of eastern Pacific depression formation, regardless of latitude, and the one Atlantic storm that unambigously formed from an African wave during 1991 (Avila and Pasch 1992). Figure 5a shows that waves leave Africa with great regularity, as has been noted previously (e.g., Simpson et al. 1968; Frank 1970; Avila and Pasch 1992). Although interpretation is somewhat subjective as to what constitutes a continuous wave track (see discussion by Molinari et al. 2000), there is reasonably good evidence that most or all eastern Pacific storms can be tracked back to Africa in the bandpass v component. Virtually all eastern Pacific tropical depression formations are preceded by disturbance growth upstream. During each active period in the eastern Pacific, new depressions tend to form progressively farther east than the previous ones, consistent with the eastward shift of the convectively active part of the MJO discussed earlier (Fig. 4) during the first active period.

Figure 5b shows the variance of the 2–6-day v component (i.e., the square of the field in Fig. 5a). This allows the amplitude of waves to be more clearly depicted. Although time variations in disturbance amplitude occur at the African coast (about 17°W at these latitudes), these variations do not correspond in a one-to-one fashion with wave amplitude or tropical depression formation in the eastern Pacific. Only once during the summer does a tropical depression form within a wave that maintains its intensity across the Caribbean and into the eastern Pacific (tropical depression 5 on 29 Jun). In July a series of strong waves leaves Africa, but their amplitude decreases in the Caribbean, and only certain waves can be extrapolated downstream to cyclogenesis locations in the eastern Pacific. Rather, it is argued following Molinari et al. (1997) and MH that the MJO-influenced wave growth in the western Caribbean and/or eastern Pacific is the dominant factor in whether eastern Pacific tropical cyclones develop.

As noted earlier, the v-component fields from the gridded global analyses are not sufficiently reliable to give a perfect measure of the wave evolution as it traverses the Atlantic. Instead, Fig. 6 shows latitude–time series of OLR for three longitudes: 75°, 90°, and 100°W. Active and inactive periods in the eastern Pacific, using the criterion of MH, are indicated. OLR is shaded every 30 W m^{-2} below 210 W m^{-2}. Regions with OLR below the latter value will be considered to have active deep convection.

Along 75°W (Fig. 6a), the active and inactive MJO periods show clearly, even though those periods are defined based on the zonal wind anomaly west of 90°W. This is expected from the anomaly fields of MH, who showed that the MJO influence extended to the western Caribbean. During active periods convection at 75°W is both more intense and more widespread than during inactive periods. Most of this convection occurs between 5° and 10°N, which is either within or just west of some of the highest peaks in the Andes. Only rarely does the active convection extend northward into the central Caribbean. During both active and inactive pe-

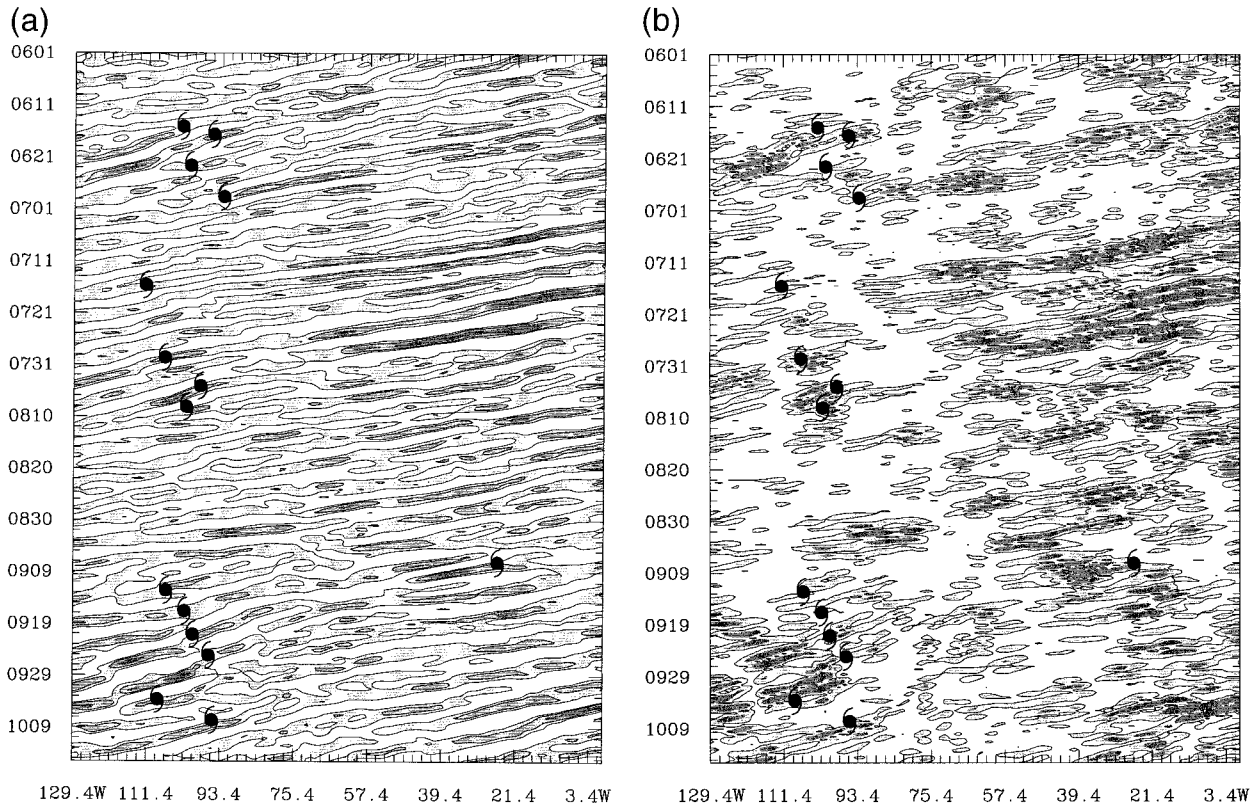

FIG. 5. Longitude–time series of (a) the bandpass (2–6 day) v component of the wind at 700 mb, averaged between 10.125° and 12.375°N, and (b) the square of the field in (a). Tropical cyclone symbols indicate the time and longitude of tropical depression formation, regardless of latitude. In (a), only the 0 and 2 m s^{-1} contours are shown; negative values are not contoured. Shading, from light to dark, represents 0–2, 2–4, and >4 m s^{-1}, respectively. In (b), only the 2 m^2 s^{-2} contour is shown; shading represents 2–8 and >8 m^2 s^{-2}, respectively.

riods, OLR varies in time on the scale of waves in the easterlies, suggesting, as does the v-component longitude–time series in Fig. 5, that waves are continually propagating through the region. If a wave passage is defined by OLR falling below, then back above, 210 W m^{-2}, then 30–35 wave passages can be defined along 75°W, depending on the latitude chosen, giving a wave period of approximately 4 days.

Along 90°W (Fig. 6b), active and inactive periods again show well in the OLR, and the regular passage of waves in the easterlies also shows. One variation from 75°W is that convection no longer occurs within 300 km of the equator, and occurs much more extensively between 10° and 15°N. The lack of equatorial convection relates to the cold water in this region at 90°W. The strong convection farther north relates to the high sea surface temperature there.

At 100°W (Fig. 6c) the negative OLR anomalies are much stronger than at 90°W while still fluctuating on a 4–5-day timescale. This suggests indirectly that waves are continuing to intensify as they move westward. Also shown in Fig. 6c are the latitudes of tropical depression formation, regardless of their longitude. The northward progression of depression formations previously shown in Fig. 4 occurs during each active period of the MJO.

Although it is difficult to discern in Fig. 6 owing to the time axis scaling, higher OLR at 12°–15°N often lags that near and south of the mean ITCZ. This indicates a SW–NE tilt to the waves, consistent with that found by Molinari et al. (2000). This tilt is expected for unstable waves growing south of the jet and, thus, provides indirect support for the modal instability arguments of Molinari et al. (1997).

In summary, synoptic-scale easterly waves can be tracked from Africa across the Atlantic in the bandpass v component. Little correlation exists between the strength of waves in the eastern Atlantic and the frequency of tropical cyclogenesis in the eastern Pacific. Rather, convective anomalies on the wave scale intensify as they pass through the western Caribbean and eastern Pacific during active periods. The results suggest that during the 1991 season tropical cyclogenesis is strongly influenced by the MJO via its interaction with the regular progression of westward-moving waves in the easterlies.

5. Role of the eastern Pacific ITCZ in cyclogenesis

If the ITCZ were an east–west line of steady convection at a fixed latitude, it would appear as a horizontal

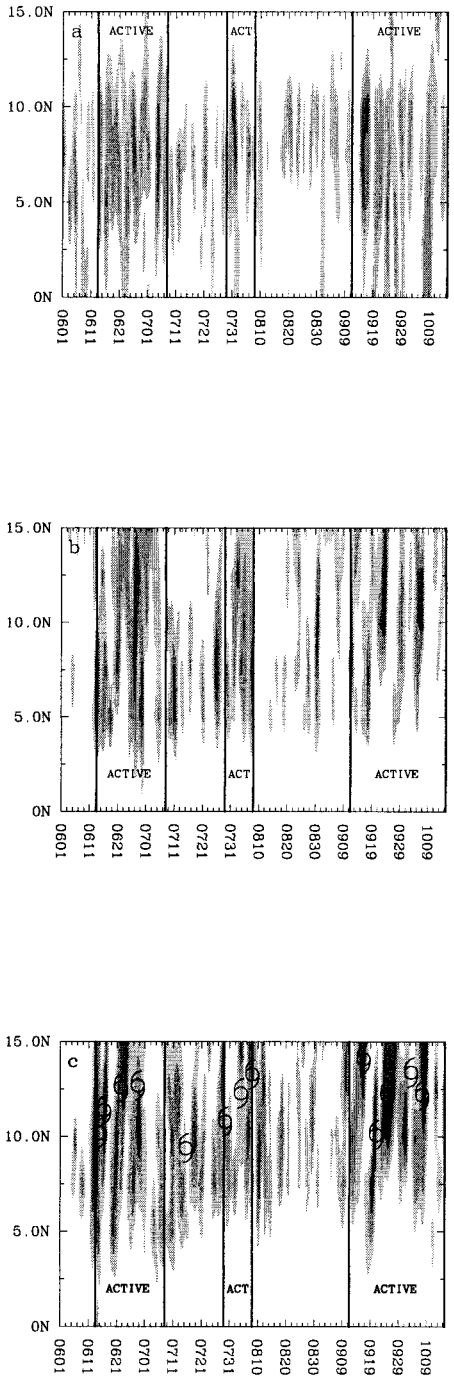

FIG. 6. Latitude–time series of OLR, filtered to remove the diurnal cycle, at (a) 75°, (b) 90°, and (c) 100°W. Shading, from light to dark, represents 180–210, 150–180, and <150 W m^{-2}, respectively. Active periods defined by the criterion of MH (their Fig. 1) are indicated. In (c), the latitudes and times of formation of eastern Pacific tropical depressions, regardless of longitude, are indicated by the tropical cyclone symbols. Tropical depression 10 (see Table 1) is not shown because it formed north of the top latitude in the figure.

strip across each panel in Fig. 6. It is apparent that little such steadiness occurs. If instead the ITCZ were a narrow band of convection that slowly oscillated meridionally, it would appear as a sinusoidal band in Fig. 6. This behavior also does not occur. Instead, (i) convection varies predominantly on the timescale of waves in the easterlies (which in turn are modulated by the MJO), and (ii) the meridional scale of convection during active periods is 500–1000 km. Both in time and in meridional extent, it appears that the wave scale dominates the OLR variability, and no narrow strip corresponding to the mean structure in Fig. 2 appears in Fig. 6.

In contrast, the lowpass-filtered 1000-mb vorticity maxima in Fig. 4 show a coherent, simply connected ITCZ the vast majority of the time. As noted earlier, this feature shifts northward during the active period, then breaks up to the north and redevelops to the south near its original latitude. Figure 4 also shows that tropical depressions form very near this lowpass-filtered ITCZ. The ITCZ may be considered a slowly varying background through which the waves propagate, and within which tropical depression formation is focused.

Lowpass-filtered OLR in Fig. 4, however, often behaves differently than 1000-mb vorticity and thus complicates the interpretation. During an inactive MJO, a well-defined strip of low OLR nearly coincides with the strip of maximum vorticity, and the ITCZ definition is unambiguous. In constrast, during active MJO phases the region of deep convection expands northward and covers a much larger area than during inactive MJO periods. The meaning of the ITCZ under such circumstances is not altogether certain. If the ITCZ definition is unclear, it becomes rather difficult to discuss its role in cyclogenesis.

Zehnder et al. (1999) examined idealized simulations in the eastern Pacific that contained an upstream wave, the influence of idealized mountains resembling those in Central America, and a preexisting ITCZ. Significant growth of the upstream waves on the scale of incipient tropical depressions occurred only when the ITCZ was included in the experiments. The interactions were complex, in that removing the influence of either the upstream wave or the orography eliminated significant disturbance growth even when the ITCZ was present. When all three elements were present, the ITCZ developed a waviness, but the concurrent meridional shifts were far less than those shown in Fig. 4.

The ECMWF gridded analyses do not incorporate sufficient data to meaningfully describe the flow evolution on the timescale of Zehnder et al.'s (1999) results. In addition, the well-defined, zonally oriented ITCZ in their simulations may often not be present. As a result, the exact nature of the interactions between easterly waves, the MJO, and the ITCZ, and their role in eastern Pacific tropical cyclogenesis, remains a fruitful topic for research.

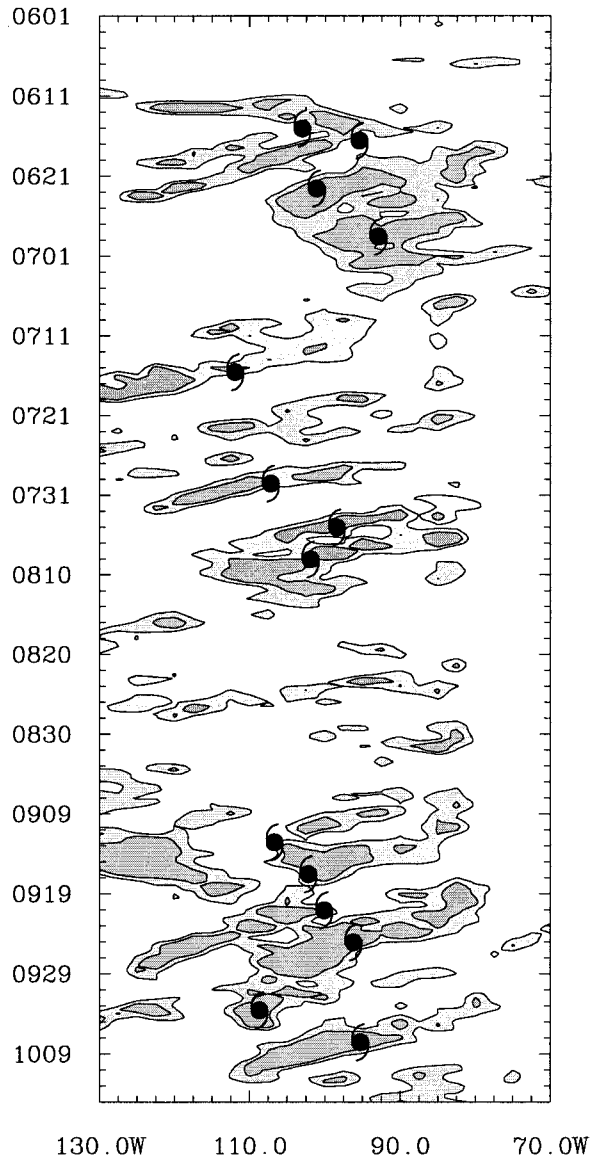

FIG. 7. Longitude–time series of OLR during the summer and early fall of 1991, filtered to remove the diurnal cycle and averaged from 12.5° to 15N. Only contours <210 W m^{-2} are shown. The contour increment is 30 W m^{-2}. Light shading, 180–210 W m^{-2}; dark shading, <180 W m^{-2}.

6. Discussion

Figure 7 provides a means of synthesizing the planetary- and synoptic-scale influences on eastern Pacific tropical cyclogenesis. It shows a Hovmöller diagram of OLR, filtered only to remove the diurnal mode, for a region from the central Caribbean to 130°W, averaged from 12.5° to 15°N (north of the mean ITCZ latitude). Little convection occurs upstream of central America because the Caribbean is relatively dry. Figure 7 shows the eastward-propagating MJO superclusters on the large scale and the growth of convection within westward-propagating easterly waves as they cross into the favorable part of the MJO.

Figures 5, 6c, and 7 show a general eastward and northward shift of tropical depression formation as the MJO-related active period evolves. The eastward shift most likely relates to the motion of the MJO, although Rossby wave radiation from each hurricane vortex (Holland 1995) cannot be ruled out. If the ITCZ is defined by its lowpass-filtered vorticity maxima near the surface, the northward shift of tropical cyclone genesis relates to analogous motion of the ITCZ.

The results of this and previous studies (MH; Molinari et al. 1997, 2000) suggest that a prominent mode of cyclogenesis in the eastern Pacific occurs as follows: (i) the convectively active phase of the MJO moves into the region from the west; (ii) the meridional PV gradient sign reversal becomes strong in the western Caribbean and eastern Pacific; (iii) upstream waves, most likely from Africa, grow in intensity in the unstable region [this could occur via modal instabilities, as suggested by Molinari et al. (1997), or by nonmodal growth described by Sobel and Bretherton (1999) and by E. D. Maloney 2000, personal communication)]; and (iv) tropical depressions form in association with these growing waves, within a northward shifting ITCZ. Of course, the details of the last two steps are anything but trivial, particularly with regard to the role of the ITCZ. Nevertheless, it is argued that the planetary scale strongly influences the likelihood of genesis in the eastern Pacific, as has been argued previously by Molinari et al. (1997) and MH.

Figure 7 shows only a single season in which tropical cyclogenesis varied strongly on the scale of the MJO. During other seasons the MJO influence is not so obvious. The work of MH, however, indicates that if the MJO active and inactive periods are defined appropriately in terms of the EOFs of the near-equatorial zonal wind, the MJO can be seen to have a strong overall influence; their study encompassed 16 yr of data. An example of another year like 1991 is shown in Fig. 8, which shows the same field as in Fig. 7 but for 1983. During this El Niño year, the areal coverage of convection was larger, but a similar signature to that in 1991 appears. The active periods include early June, all of July, and mid-August to mid-September. Tropical cyclogenesis again tends to occur farther eastward with time during an active period. The major exception appears to be the October storms, but even these may have developed from waves that previously encountered the favorable MJO envelope when they were farther upstream.

Easterly waves are often given little or no role in western Pacific cyclogenesis (e.g., McBride 1995). Nevertheless, considerable evidence has been presented in the literature to support a similar mechanism to that described here. Figures 7 and 8 are consistent with the findings of Yamazaki and Murakami (1989) and Liebmann et al. (1994), and resemble the schematic of Tak-

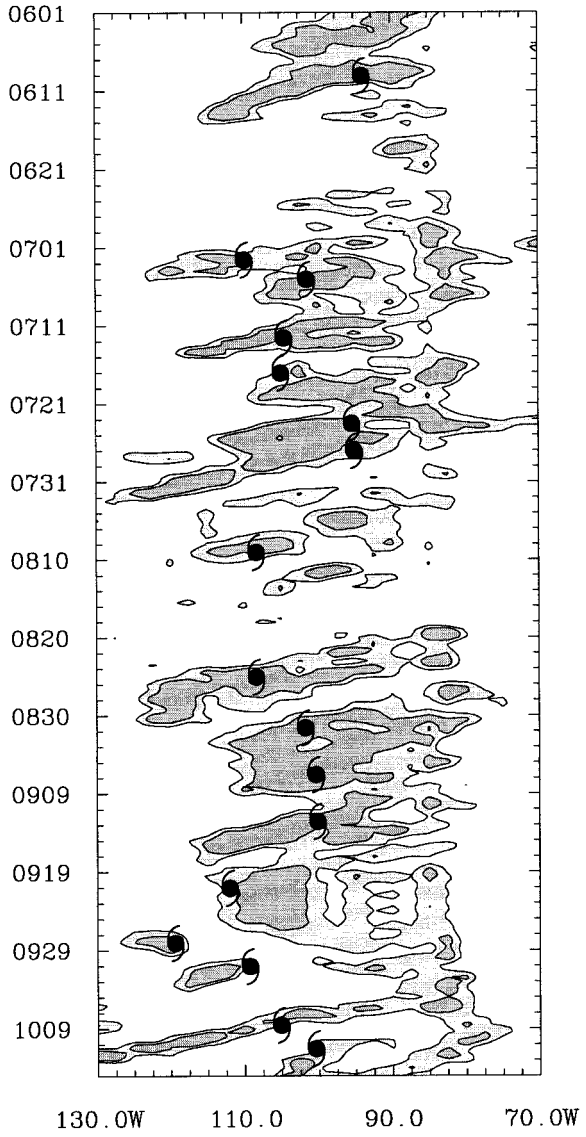

FIG. 8. As in Fig. 7 but for 1983.

ayabu and Murakami (1991); all of these studies were for the western Pacific. Further support for easterly wave involvement in the western Pacific comes from the schematic of Zehr (1992, Fig. 5.14), which shows depression development in association with an easterly wave that is approaching the westerlies of the monsoon trough. Ritchie and Holland (1999) found that approximately half of western Pacific tropical cyclones formed in association with easterly waves, the majority of which were approaching the monsoon trough. Sobel and Bretherton (1999) found that the region in which easterlies meet the monsoon westerlies in the western Pacific is favorable for easterly wave growth by a wave accumulation mechanism (see also Holland 1995). Finally, Murakami et al. (1984) showed evidence in v-component Hovmöller diagrams that waves from Africa could be tracked all the way to the western Pacific at 850 mb. Based on this evidence, it is hypothesized that the interaction of the eastward-moving MJO and westward-moving easterly waves from upstream might frequently be associated with tropical cyclogenesis in the western Pacific. This speculation will be investigated in future work.

Acknowledgments. Gridded analyses produced by ECMWF were obtained from the National Center for Atmospheric Research, which is supported by the National Science Foundation. The outgoing longwave radiation data of Liebmann and Smith (1996) were obtained electronically; we thank Catherine Smith of the University of Colorado for her assistance in this process. Positions of eastern Pacific tropical cyclones were obtained electronically from the National Hurricane Center (NHC). We thank Lixion Avila and Richard Pasch of NHC for providing additional information on eastern Pacific tropical depressions 5 and 10. This work is supported by National Science Foundation Grant ATM-9900671 and Office of Naval Research Grant N00014-98-10599.

REFERENCES

Avila, L. A., and R. J. Pasch, 1992: Atlantic tropical systems of 1991. *Mon. Wea. Rev.*, **120,** 2688–2696.

Bister, M., and K. A. Emanuel, 1997: The genesis of Hurricane Guillermo: TEXMEX analyses and a modeling study. *Mon. Wea. Rev.,* **124,** 2662–2682.

Bracken, W. E., 1999: A multiscale examination of tropical cyclogenesis. Ph.D. dissertation, University at Albany, 340 pp. [Available from Dept. Earth Atmos. Sci., Univ. at Albany, State Univ. of N.Y., 1400 Washington Ave., Albany, NY 12222.]

Farfan, L. M., and J. A. Zehnder, 1997: Orographic influence on the synoptic-scale circulations associated with the genesis of Hurricane Guillermo (1991). *Mon. Wea. Rev.,* **125,** 2683–2698.

Ferreira, R. N., W. H. Schubert, and J. J. Hack, 1996: Dynamical aspects of twin tropical cyclones associated with the Madden–Julian oscillation. *J. Atmos. Sci.,* **53,** 929–945.

Frank, N. L., 1970: Atlantic tropical systems of 1969. *Mon. Wea. Rev.,* **98,** 307–314.

Frank, W. M., 1987: Tropical cyclone formation. *A Global View of Tropical Cyclones,* R. L. Elsberry, Ed., Naval Postgraduate School, 53–90.

Gray, W. M., 1979: Hurricanes: Their formation, structure, and likely role in the tropical circulation. *Meteorology Over the Tropical Oceans,* D. B. Shaw, Ed., Royal Meteorological Society, 155–218.

Gruber, A., and J. S. Winston, 1978: Earth–atmosphere radiative heating based on NOAA scanning radiometer measurements. *Bull. Amer. Meteor. Soc.,* **59,** 1570–1573.

Harr, P. A., M. S. Kalafsky, and R. L. Elsberry, 1996: Environmental conditions prior to formation of a midget tropical storm during TCM-93. *Mon. Wea. Rev.,* **124,** 1693–1710.

Hartmann, D. L., M. L. Michelsen, and S. A. Klein, 1992: Seasonal variations of tropical intraseasonal oscillations: A 20–25-day oscillation in the western Pacific. *J. Atmos. Sci.,* **49,** 1277–1289.

Holland, G. J., 1995: Scale interaction in the western Pacific monsoon. *Meteor. Atmos. Phys.,* **56,** 57–79.

Liebmann, B., and C. A. Smith, 1996: Description of a complete (interpolated) outgoing longwave radiation dataset. *Bull. Amer. Meteor. Soc.,* **77,** 1275–1277.

——, H. H. Hendon, and J. D. Glick, 1994: The relationship between

tropical cyclones of the western Pacific and Indian Oceans and the Madden–Julian oscillation. *J. Meteor. Soc. Japan,* **72,** 401–411.

Madden, R. A., and P. R. Julian, 1994: Observations of the 40–50-day tropical oscillation—A review. *Mon. Wea. Rev.,* **122,** 814–837.

Magaña, V., J. A. Amador, and S. Medina, 1999: The midsummer drought over Mexico and Central America. *J. Climate,* **12,** 1577–1588.

Maloney, E. D., and D. L. Hartmann, 2000: Modulation of eastern North Pacific hurricanes by the Madden–Julian oscillation. *J. Climate,* **13,** 1451–1460.

Matthews, A. J., J. M. Slingo, B. J. Hoskins, and P. M. Inness, 1999: Fast and slow Kelvin waves in the Madden–Julian oscillation of a GCM. *Quart. J. Roy. Meteor. Soc.,* **125,** 1473–1498.

McBride, J. L., 1995: Tropical cyclone formation. *Global Perspectives on Tropical Cyclones,* R. Elsberry, Ed., WMO No. TCP-38, 63–105.

——, and R. Zehr, 1981: Observational analysis of tropical cyclone formation. Part II: Comparison of non-developing versus developing systems. *J. Atmos. Sci.,* **38,** 1132–1151.

Molinari, J., and D. Vollaro, 1990: External influences on hurricane intensity: Part II. Vertical structure and response of the hurricane vortex. *J. Atmos. Sci.,* **47,** 1902–1918.

——, ——, and F. Robasky, 1992: Use of ECMWF operational analyses for studies of the tropical cyclone environment. *Meteor. Atmos. Phys.,* **47,** 127–144.

——, D. Knight, M. Dickinson, D. Vollaro, and S. Skubis, 1997: Potential vorticity, easterly waves, and tropical cyclogenesis. *Mon. Wea. Rev.,* **125,** 2699–2708.

——, D. Vollaro, S. Skubis, and M. Dickinson, 2000: Origins and mechanisms of eastern Pacific tropical cyclogenesis: A case study. *Mon. Wea. Rev.,* **128,** 125–139.

Murakami, T., T. Nakazawa, and J. He, 1984: On the 40–50 day oscillations during the 1979 Northern Hemisphere summer. *J. Meteor. Soc. Japan,* **62,** 440–468.

Rappaport, E. N., and M. Mayfield, 1992: Eastern North Pacific hurricane season of 1991. *Mon. Wea. Rev.,* **120,** 2697–2708.

Raymond, D. L., C. López-Carrillo, and L. López Cavazos, 1998: Case-studies of developing east Pacific easterly waves. *Quart. J. Roy. Meteor. Soc.,* **124,** 2005–2034.

Ritchie, E. R., and G. J. Holland, 1993: On the interaction of tropical-cyclone-scale vortices. I: Observations. *Quart. J. Roy. Meteor. Soc.,* **119,** 1363–1380.

——, and ——, 1999: Large-scale patterns associated with tropical cyclogenesis in the western Pacific. *Mon. Wea. Rev.,* **127,** 2027–2043.

Schubert, W. H., P. E. Ciesielski, D. E. Stevens, and H. Kuo, 1991: Potential vorticity modeling of the ITCZ and the Hadley circulation. *J. Atmos. Sci.,* **48,** 1493–1509.

Simpson, J., E. Ritchie, G. J. Holland, J. Halverson, and S. Stewart, 1997: Mesoscale interactions in tropical cyclone genesis. *Mon. Wea. Rev.,* **125,** 2643–2661.

Simpson, R. H., N. Frank, D. Shideler, and H. M. Johnson, 1968: Atlantic tropical disturbances, 1967. *Mon. Wea. Rev.,* **96,** 251–259.

Sobel, A. H., and C. S. Bretherton, 1999: Development of synoptic-scale disturbances over the summertime tropical northwest Pacific. *J. Atmos. Sci.,* **56,** 3106–3127.

Takayabu, Y. N., and M. Murakami, 1991: The structure of super cloud clusters observed in 1–20 June 1996 and their relationship to easterly waves. *J. Meteor. Soc. Japan,* **69,** 105–125.

Tomas, R. A., and P. J. Webster, 1997: The role of inertial instability in determining the location and strength of near-equatorial convection. *Quart. J. Roy. Meteor. Soc.,* **123,** 1445–1482.

——, J. R. Holton, and P. J. Webster, 1999: The influence of cross-equatorial pressure gradients on the location of near-equatorial convection. *Quart. J. Roy. Meteor. Soc.,* **125,** 1107–1128.

Weickmann, K. M., G. N. Kiladis, and P. D. Sardeshmukh, 1997: The dynamics of intraseasonal atmospheric angular momentum oscillations. *J. Atmos. Sci.,* **54,** 1445–1461.

Yamazaki, N., and M. Murakami, 1989: An intraseasonal amplitude modulation of the short-term tropical disturbances over the western Pacific. *J. Meteor. Soc. Japan,* **67,** 791–807.

Zehnder, J. A., 1991: The interaction of planetary-scale tropical easterly waves with topography: A mechanism for the initiation of tropical cyclones. *J. Atmos. Sci.,* **48,** 1217–1230.

——, D. M. Powell, and D. L Ropp, 1999: The interaction of easterly waves, orography, and the intertropical convergence zone in the genesis of eastern Pacific tropical cyclones. *Mon. Wea. Rev.,* **127,** 1566–1585.

Zehr, R. M., 1992: Tropical cyclogenesis in the western north Pacific. NOAA Tech. Rep. NESDIS 61, 181 pp. [Available from National Technical Information Service, 5285 Port Royal Road, Springfield, VA 22161.]